

Work function and induced band bending characterization for engineering of selective contact for solar cells

Marshall Wilson^{1*}, Alexandre Savtchouk¹, Ziv Hameiri², Jie Cui³ and Jacek Lagowski¹

¹Semilab SDI, Tampa, FL 33617, USA

²University of New South Wales (UNSW), Sydney NSW 2052, Australia

³Australian National University (ANU), Canberra ACT 0200, Australia

*Corresponding author

DOI: 10.5185/amlett.2018.2084

www.vbripress.com/aml

Abstract

This work demonstrates the effectiveness of non-contact Kelvin-probe and surface photo voltage characterization of the work function (WF) induced barriers formed in silicon (Si) by thin 5nm carrier selective contact films of MoO_x, TiO₂ and MgF₂. The calibrated Kelvin probe in the dark and under strong illumination were used to determine the dark WF of the deposited films and the band bending in the Si, $\Phi_{BB} = \text{WF}_{\text{Dark}} - \text{WF}_{\text{Light}}$. The ac-surface photo voltage provided an independent measurement of the Si depletion layer width. Whole wafer mapping of all parameters can be performed. For n-type Si the high work function oxides MoO_x (WF~5.7eV) and TiO₂ (WF~5.0eV) are found to induce a depletion barrier with the height increasing with WF as $\Phi_{BB}[\text{eV}] = 0.23\text{WF} - 0.77$, i.e. quite similar to the well-known relationship for metal-silicon contacts. For the low work function MgF₂ film, a depletion barrier was induced only in p-type Si. For this case, full wafer mapping revealed a lower WF pattern coinciding with larger band bending giving the slope, $\Delta\Phi_{BB}/\Delta\text{WF} \sim -0.52$. The slopes of 0.23 and 0.52 for n- and p-type Si deviate significantly from the ideal slope of 1. This result implies that the barrier formation at the Film-Si heterojunction is limited by the effect of interfacial layers and interface states in analogy to the well-known effects in Metal-Si contacts. It is believed that this demonstrated very fast, preparation-free, non-contact characterization technique can benefit research and engineering of selective contacts for solar cells. Copyright © 2018 VBRI Press.

Keywords: Solar cell, work function, band bending, hole selective contacts, electron selective contacts.

Introduction

One of the critical factors in achieving high efficiencies in state-of-the-art Si solar cells is maximizing carrier collection at the contacts with the silicon absorber. To achieve that goal, high and low work function (WF) materials or materials with a suitable band offset with silicon have been recently investigated for use as dopant-free carrier selective contacts in silicon solar cells. For hole selective contacts, the research has been focused on transition metal oxides (TMOs) with high work functions such as MoO_x [1-6], VO_x [7,8] and WO_x [5,8], while for electron selective contacts TiO₂ [9,10] with a small conduction band offset with silicon and low work function alkali metal salts such as LiF [11] and MgF₂ [12] have been investigated.

Sufficiently high (for hole selective contacts) or low (for electron selective contacts) work function materials induce band bending in the silicon absorber that acts as a rectifying barrier to carrier flow. Thus, this band bending is a critical parameter for carrier selective contacts giving important information on effective work function and interfacial charges that may influence the induced barrier. A number of recent investigations have

used a contact surface photo voltage (SPV) technique for measurement of this induced band bending for hole selective contact materials [3-5].

In this work we propose the use of a non-contact Kelvin-probe measurement of work function and surface photo voltage measurement of induced band bending to characterize carrier selective contact films. Preparation-free, quick feedback results of work function and band bending can be extremely useful in characterizing these carrier selective films. Full wafer mapping Kelvin probe measurements of the work function and band bending can also be used for optimizing non-uniformities in these carrier selective contact films.

Experimental

The samples studied in this work include 50nm thick films of MoO_x, TiO₂ and MgF₂ on mono-crystalline silicon n-type and p-type wafers with a dopant concentration around 2 to 3x10¹⁷ cm⁻³. The MoO_x and MgF₂ films were thermally evaporated from a powder source, while the TiO₂ film was deposited by atomic layer deposition.

The Kelvin probe measurements were performed using the Semi lab PV-2000A metrology tool [13]. In a Kelvin probe measurement, an electrode, sitting a distance of $\sim 250\mu\text{m}$ above the sample, vibrates with a frequency, ω , modulating the electrode-wafer capacitance and generates a current, $J(t) = \Delta C \omega (V_{CPD} + V_{DC}) \cos(\omega t)$; where V_{CPD} is the contact potential difference between the electrode and the semiconductor. A compensation mode is used in which a DC bias, V_{DC} , is applied between the electrode and the wafer until the current $J(t)$ goes to zero (e.g., $V_{DC} = -V_{CPD}$). By nulling the current ($J = 0$) one obtains the contact potential difference value V_{CPD} . It is a common practice to simply refer to the contact potential difference value as “surface voltage”, V , instead of V_{CPD} . The measured V_{CPD} value is equal to the work function difference between the sample (ϕ_s) being measured and the metal (ϕ_m) of Kelvin probe electrode ($V_{CPD} = \phi_m - \phi_s$). For absolute work function (WF) measurements, the offset of the Kelvin-probe electrode (gold) is calibrated using a Ag/AgCl reference half-cell. Band bending in Si, critical for selective contacts, was measured as the difference between work function in the dark and under strong illumination, $\Phi_{BB} = \text{WF}_{\text{Dark}} - \text{WF}_{\text{Light}}$. Small signal surface photo voltage (ac-SPV) was used to identify band bending and measure the depletion layer width.

Results and discussion

Fig. 1 shows correlation between the Kelvin-probe measured WF in a cleanroom ambient and literature values, measured with ultraviolet photoelectron spectroscopy (UPS) under vacuum, confirming the WF range provided by the samples [1,9,12]. The work function for n- and p-type Si with a dopant concentration of about $3 \times 10^{17} \text{ cm}^{-3}$ is: $\text{WF}_{\text{n-Si}} = 4.2\text{eV}$ for n-type Si and $\text{WF}_{\text{p-Si}} = 5.05\text{eV}$ for p-type Si. To induce a depletion barrier in n-type Si, the work function of the film material should be larger than 4.2eV ($\text{WF}_{\text{film}} > \text{WF}_{\text{n-Si}}$). This is satisfied for TiO_2 and MoO_x but not for MgF_2 . For p-type Si the necessary condition for formation of the induced depletion barrier is $\text{WF}_{\text{film}} < \text{WF}_{\text{p-Si}}$. Considering the $\text{WF}_{\text{p-Si}}$ of about 5.05eV , this condition is satisfied only for the MgF_2 film.

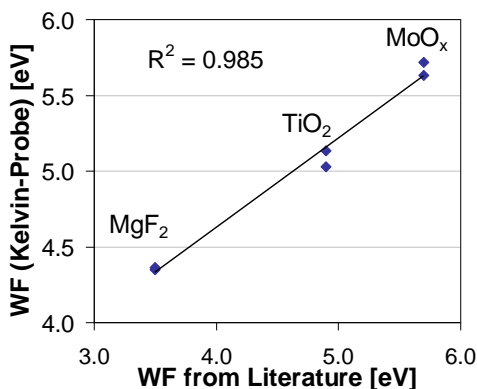


Fig. 1. Correlation of work function estimated from surface voltage with literature work function values for MgF_2 , TiO_2 and MoO_x films on n-type substrates.

The band bending results in Fig. 2 for n-type Si confirm that depletion type band bending is induced only by the high work function MoO_x and TiO_2 films. Due to its high work function MoO_x acts as a hole selective contact, however in spite of its high work function TiO_2 actually acts as an electron selective contact due to its large valence band offset ($\Delta E_V = \sim 2.0\text{eV}$) and small conduction band offset ($\Delta E_C = \sim 0.05\text{eV}$) with the silicon absorber [9]. No band bending is seen for the lower work function MgF_2 film that on n-Si is suitable for ohmic rather than selective contact. Results of ac-SPV in Fig. 3 support the band bending behaviors. The increase of ac-SPV for the high work function material is due to a larger increase in the width of the depletion layer. The largest width is for the MoO_x film. No depletion barrier was observed for the MgF_2 film on n-type Si. However, for MgF_2 a depletion band bending is induced on p-type Si. In this case MgF_2 can be used as an electron selective contact.

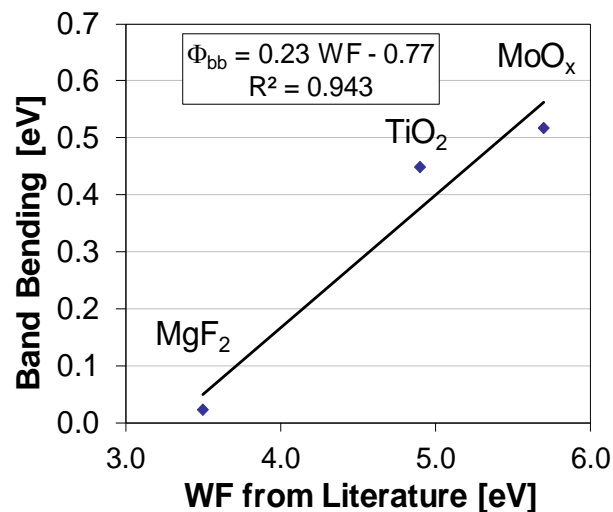


Fig. 2. Correlation of band bending (V_{SB}) with literature work function values for MgF_2 , TiO_2 and MoO_x films on n-type substrates.

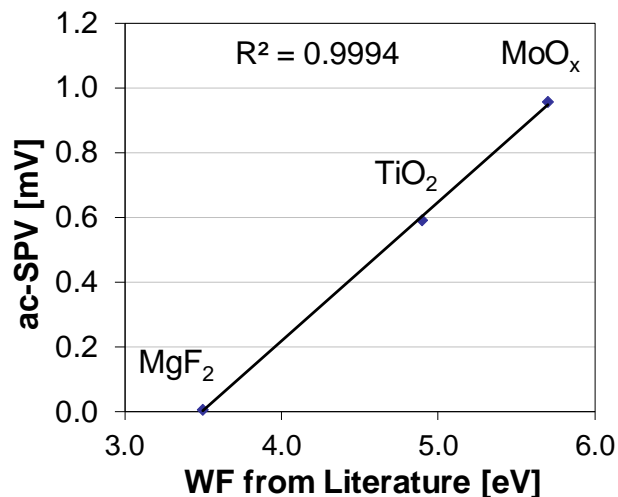


Fig. 3. Correlation of ac-SPV signal with literature work function values for MgF_2 , TiO_2 and MoO_x films on n-type substrates.

A corresponding (Φ_{BB} , WF) correlation is evident in the Kelvin-probe wafer maps of WF and Φ_{BB} in Fig. 4A and Fig. 4B, respectively, where low WF corresponds to high Φ_{BB} . Comparing the same wafer sites, the correlation plot in Fig. 5 is obtained, indicating a linear increase of band bending with decreasing work function. Utilizing full wafer mapping allows for such quantitative correlations while minimizing the need for a large number of samples with different work functions. It is of significance to note that the experimental slopes ($\Delta\Phi_{BB}/\Delta WF$) of 0.23 and -0.52 for n-type and p-type Si, respectively, are substantially lower than an ideal 1:1 correlation. Such a 1:1 correlation corresponds to the case when the WF difference between the film and Si is completely accommodated in the Si surface barrier, $\Phi_{BB} = WF_{\text{film}} - WF_{\text{Si}}$. According to the Cowley and Sze model of work function induced barrier heights in semiconductors [14], the low slope value is indicative of the limitations due to high interface trap density with additional contributions from interfacial dipole layers and charge on the film. Engineering of selective contacts for solar cells incorporates interface passivation layers to reduce the above limitations.

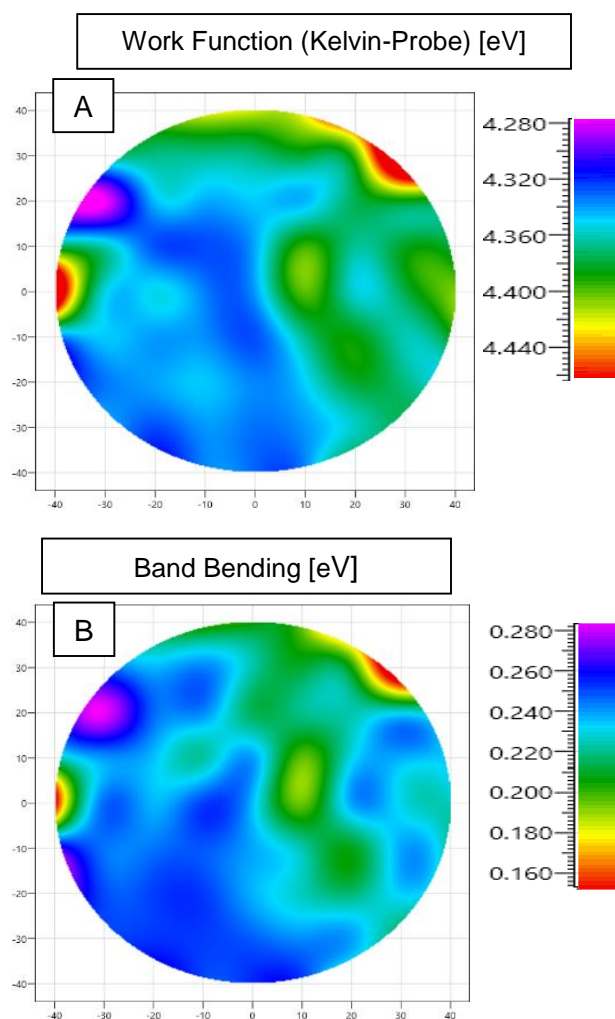


Fig. 4. Kelvin probe measured map of work function estimated from surface voltage (A) and band bending (B) for a MgF₂ film on a p-type substrate.

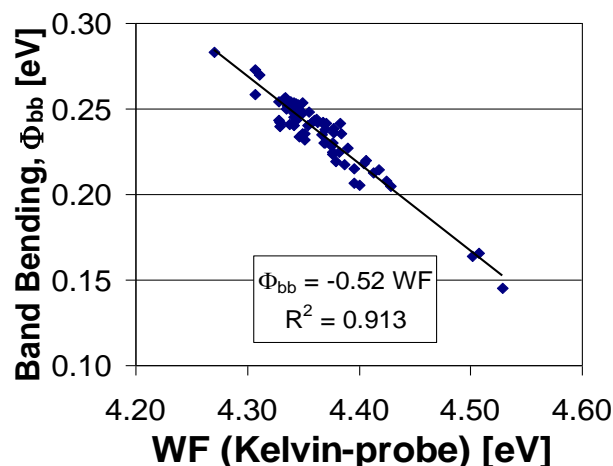


Fig. 5. Site by site correlation of Kelvin probe measured work function and band bending for the maps presented in Figures 4A and 4B for the MgF₂ film.

Conclusion

The presently demonstrated very fast, non-contact, non-invasive Kelvin probe characterization approach can benefit both fundamental understanding and practical implementation of work function based solar cell engineering of carrier selective contacts. Additionally, this approach can be easily applied to passivated contact work function engineering in organic solar cells.

References

- Meyer J.; Hamwi S.; Kroger M.; Kowalsky W.; Riedl T.; Kahn A.; *Adv. Mater.*, **2012**, *24*(40), 5408–5427.
- Battaglia C.; Yin X.; Zheng M.; Sharp I.D.; Chen T.; McDonnell S.; Azcatl A.; Carraro C.; Ma B.; Maboudian R.; Wallace R.M.; Javey A.; *Nano Lett.*, **2014**, *14*, 967-71.
- Geissbuhler J.; Werner J.; Nicolas S.M.; Barraud L.; Hessler-Wyser A.; Despeisse M.; Nicolay S.; Tomasi A.; Niesen B.; De Wolf S.; Ballif C.; *Appl. Phys. Lett.*, **2015**, *107*, 081601.
- Bivour M.; Temmler J.; Steinkemper H.; Hermle M.; *Solar Energy Materials and Solar Cells*, **2015**, *142*, 34-41.
- Bivour M.; Macco B.; Temmler J.; Kessels W.M.; Hermle M.; *Energy Procedia*, **2016**, *92*, 443-449.
- Neusel L.; Bivour M.; Hermle M.; *Energy Procedia*, **2017**, *124*, 425-434.
- Gerling L.G.; Masmitja G.; Voz C.; Ortega P.; Puigdollers J.; Alcobilla R.; *Energy Procedia*, **2016**, *92*, 633-637.
- Gerling, L.G.; Mahato S.; Morales-Vilches A.; Masmitja G.; Ortega P.; Voz C.; Alcobilla R.; Puigdollers J.; *Solar Energy Materials and Solar Cells*, **2016**, *145*, 109-115.
- Avasthi S.; McClain W.E.; Man G.; Kahn A.; Schwartz J.; Sturm J.C.; *Appl. Phys. Lett.*, **2013**, *102*(20), 203901.
- Yang X.; Weber K.; Hameiri Z.; De Wolf S.; *Prog. Photovolt: Res. Appl.*, **2017**, *25*, 896-904.
- Zhang Y.F.; Liu R.Y.; Lee S.T.; Sun B.Q.; *Appl. Phys. Lett.*, **2014**, *104*, 083514.
- Wan Y.M.; Samundsett C.; Bullock J.; Allen T.; Hettick M.; Yan D.; Zheng P.T.; Zhang X.Y.; Cui J.; McKeon J.; Javey A.; Cuevas A.; *ACS Appl. Mat. Interface*, **2016**, *8*(23), 14671-14677.
- Findlay A.; Marinsky D.; Edelman P.; Wilson M.; Savtchouk A.; Lagowski J.; *ECS Journal of Solid State Science and Technology*, **2016**, *5*(4), P3087-P3095.
- S.M. Sze and A.M. Crowley, *Physics of Semiconductor Devices*, 3rd ed., **2006**, Chapter 3.2.3, p.142.